JOURNAL OF GUIDANCE, CONTROL, AND DYNAMICS
Vol. 24, No. 4, July–August 2001

Approximate Solutions for Tethered Satellite Motion

S. Cho*
Electronics and Telecommunications Research Institute, Taejon 305-350, Republic of Korea
and
T. A. Lovell,† J. E. Cochran Jr.,‡ and D. A. Cicci§
Auburn University, Auburn, Alabama 36849-5338

The formulation of approximate solutions to equations that embody the dominant characteristics of the orbital motion of a two-satellite tethered system are studied. The orbital motion of the system is viewed as perturbed two-body motion, and a restricted tether problem is obtained by neglecting librational motion. An exact analytical solution to this restricted problem in terms of elliptic functions is presented. An approximate solution to the restricted tether problem obtained by applying the method of averaging is also provided. An approximation for small-amplitude librational motion is formulated, whose solution is based on methods for solving equations with variable coefficients. The analytical solutions are good approximations to the orbital motion of the tether-perturbed satellite and the librational motion of the system when the libration is small. The restricted tether motion approximation is then utilized to solve the identification problem of a tethered satellite system.

Nomenclature

a^*	=	apparent semimajor axis
e^*	=	apparent eccentricity
F	=	incomplete elliptic integral of the first kind
h	=	nondimensional angular momentum
K	=	complete elliptic integral of the first kind
K'	=	associate complete elliptic integral of the first kind
k	=	modulus of Jacobian elliptic functions and integral
k'	=	complementary modulus of Jacobian elliptic functions and integral
m, m_p	=	masses of satellites
q	=	Jacobi's nome
r	=	nondimensional radial distance, radial distance/r_E
r_E	=	radius of the Earth, 6,378,000 m
sn	=	Jacobian elliptic function
t	=	time
t^*	=	nondimensional time, $t\sqrt{(\mu/r_E^3)} = t \times 0.0012394$
u	=	$1/r$
$\boldsymbol{X}$	=	state vector
$\alpha, \beta, \gamma, \xi$	=	variable coefficients
ε	=	tether parameter, $m_p\rho/(m+m_p)r_E$
θ	=	orbital angle (true anomaly)
θ_2	=	out-of-plane libration angle
θ_3	=	in-plane libration angle
μ	=	gravitational constant of the Earth
ρ	=	tether length
φ, φ^*	=	amplitudes
ω	=	orbital frequency

I. Introduction

IT is well-known that the motion of each satellite in a tethered satellite system (TSS) in the Earth's gravitational field is non-Keplerian (see Ref. 1). This characteristic may present problems to those who are detecting, identifying, and tracking space objects. Cho et al.[2] showed that identification and estimation of the states of a two-satellite tethered system by using observations of one of the satellites in the system is possible. However, they found that estimation of the librational motion by using observations over a short period of time is difficult. These results motivated Cochran et al.[3] to investigate the problem of characterizing the information available in observations of one of the satellites of a two-satellite tethered system. They showed that the magnitude of the tether parameter (a combination of the tether length and the masses of the end bodies[2]) strongly affects the conditioning of the information matrix, as does the type of observations available. The elements of the information matrix corresponding to the librational motion of the system are generally relatively small, leading to large condition numbers. Difficulties in acquiring information on librational motion have motivated a quest for analytical approximations for the orbital and librational motions of TSS.[4,5]

In this paper, a restricted tether motion equation is obtained that embodies the dominant characteristics of the orbital motion of the TSS, and approximate analytical solutions to the orbital and librational equations of motion for a TSS are presented. First, the equations that govern planar motion of a two-satellite tethered system given in Ref. 2 are discussed. These equations are then transformed by a change of variables, as in the classical two-body problem. The transformed equations are solved approximately by using a combination of methods. Comparisons of analytical results with numerical solutions are made. Then, the use of the restricted tether motion equations as part of a three-stage identification algorithm for TSS is discussed.

II. Equations of Motion

A two-satellite tethered system is depicted in Fig. 1. The vector $\boldsymbol{r}$ defines the position of satellite m with respect to the point mass Earth E, and m_p is a satellite connected to m by the tether. For the dynamic model employed herein, the mass of the tether is assumed to be distributed equally to m and m_p. General nondimensionalized equations of motion for this system were derived in Ref. 2. There it was shown that the out-of-plane librational motion of a TSS is generally small and has less effect on orbital motion than in-plane libration because the velocity it produces is orthogonal to the orbital velocity. Thus, the planar motion for satellite m can be described by the following nondimensional equations:

$$\ddot{r} = \dot{\theta}^2 r - 1/r^2 + \varepsilon\left[(\dot{\theta}_3 + \dot{\theta})^2 + (1/r^3)\left(3\cos^2\theta_3 - 1\right)\right]\cos\theta_3 \tag{1}$$

$$\ddot{\theta} = -2\dot{\theta}\dot{r}/r + \varepsilon\left[(\dot{\theta}_3 + \dot{\theta})^2 + (1/r^3)\left(3\cos^2\theta_3 - 1\right)\right]\sin\theta_3 \tag{2}$$

Relative motion of the tethered satellite m_p with respect to satellite m is described by the in-plane librational angle θ_3 as shown in

Received 26 April 1999; revision received 23 June 2000; accepted for publication 15 September 2000.

*Senior Member of Research Staff.

†Graduate Research Assistant, Department of Aerospace Engineering. Member AIAA.

‡Professor and Head, Department of Aerospace Engineering. Associate Fellow AIAA.

§Associate Professor, Department of Aerospace Engineering. Associate Fellow AIAA.

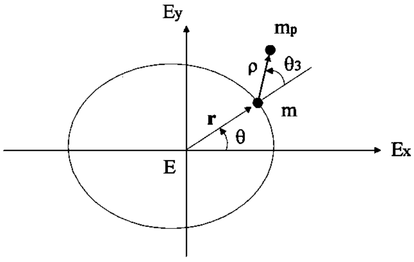

Fig. 1 TSS motion on orbit plane.

Fig. 1. The equation for the librational motion is

$$\ddot{\theta}_3 = -\ddot{\theta} - 3(1/r^3)\cos\theta_3 \sin\theta_3 \tag{3}$$

In Eqs. (1–3), $(\dot{\ }) = d(\ )/dt^*$. The tether parameter ε, defined in the Nomenclature, is a combination of a mass ratio and a nondimensional tether length ρ/r_E.

III. Tether Perturbed Motion

The terms that include the tether parameter on the right-hand side of Eqs. (1) and (2) represent forces due to the mass m_p in addition to those that cause Keplerian motion. Because the tether parameter is small, in general, we may treat the additional forces as small perturbations to the Keplerian motion of satellite m that would occur if the tether were cut. The perturbations are mainly the gravity-gradient forces due to the mass m_p. Also, the librational motion can often be considered as a perturbation, especially when the magnitude of the libration angle θ_3 is small as for a typical tethered system.

Equations (1–3) may then be transformed by replacing the variable r by $u = 1/r$ and using $h = r^2\dot{\theta}$ instead of $\dot{\theta}$, for mathematical convenience. The time variable t^* can be replaced by a timelike variable τ defined by $\dot{\tau} = hu^2$. Note that this is similar to the classical transformation made in solving the two-body problem. Then, Eqs. (1–3) can be rewritten as

$$u'' + u = 1/h^2 + \varepsilon\left[-u(\theta_3' + 1)^2 - 2/h^2\right](\theta_3 u' + u) \tag{4}$$

$$h' = \varepsilon\left[u(\theta_3' + 1)^2 + 2/h^2\right]\theta_3 h \tag{5}$$

and

$$\theta_3'' = -(2u'/u)(\theta_3' + 1) - (3/h^2 u)\theta_3 + \varepsilon\left[-u(\theta_3' + 1)^2 - 2/h^2\right]\theta_3(\theta_3' + 1) \tag{6}$$

where $(\ )' = d(\ )/d\tau$. In Eqs. (4–6), sinusoidal terms in θ_3 have been approximated by Taylor series expansions assuming a small libration angle θ_3.

Restricted Tether Orbital Motion

When librational motion is neglected, a restricted tether problem may be defined that embodies the dominant characteristics of the tether-perturbed orbital motion. Equations for the restricted tether motion are obtained by neglecting θ_3 and its derivatives in Eqs. (4) and (5):

$$u'' + u = 1/h^2 + \varepsilon(-u - 2/h^2)u \tag{7}$$

$$h' = 0 \tag{8}$$

An exact solution to the restricted tether problem may be found as follows. A first-order differential equation for u is obtained by multiplying Eq. (7) by u and integrating once:

$$u' = 2\sqrt{-\varepsilon(u^3/3) - (1 + 2\varepsilon/h^2)(u^2/2) + u/h^2 + E} \tag{9}$$

This may be rewritten as

$$\sqrt{D}\int_{\tau_0}^{\tau} d\tau = \int_{u_0}^{u} \frac{du}{\sqrt{-u^3 - (B/D)u^2 + (C/D)u + 2E/D}} \tag{10}$$

where

$$B = 1 + 2\varepsilon/h^2, \qquad D = \tfrac{2}{3}\varepsilon, \qquad C = 2/h^2$$

$$E = \frac{1}{2}\left(\frac{du}{d\tau}\right)_0 + \frac{1}{3}\varepsilon u_0^3 + \frac{1}{2}\left(1 + \frac{2}{h^2}\varepsilon\right)u_0^2 - \frac{1}{h^2}u_0$$

We can put Eq. (10) into a standard form,

$$\sqrt{D}\int_{\tau_0}^{\tau} d\tau = \int_{b}^{u} \frac{du}{\sqrt{(a-u)(u-b)(u-c)}} - \int_{b}^{u_0} \frac{du}{\sqrt{(a-u)(u-b)(u-c)}} \tag{11}$$

where a, b, and c are constants that satisfy the relation $a \geq u > b > c$. We can use elliptic functions[6] to evaluate the integral in Eq. (11). The solution is

$$\sqrt{D}(\tau - \tau_0) + gF(\varphi^*, k) = g\, sn^{-1}(\sin\varphi) \tag{12}$$

where $g = 2/\sqrt{(a-c)}$, $k^2 = (a-b)/(a-c)$, and F is the incomplete elliptic integral of the first kind. The amplitudes φ and φ^* are obtained from

$$\varphi = \sin^{-1}\left(\sqrt{\frac{(a-c)(u-b)}{(a-b)(u-c)}}\right) \tag{13}$$

$$\varphi^* = \sin^{-1}\left(\sqrt{\frac{(a-c)(u_0-b)}{(a-b)(u_0-c)}}\right) \tag{14}$$

respectively.

By using Eqs. (13) and (14), we can obtain the following expression for $u(\tau)$

$$u(\tau) = \frac{ck^2 sn^2\left[\sqrt{D}\tau/g + F(\varphi^*, k)\right] - b}{k^2 sn^2\left[\sqrt{D}\tau/g + F(\varphi^*, k)\right] - 1} \tag{15}$$

The Jacobian elliptic function $sn(\ )$ can be expressed as a rapidly convergent series expansion

$$sn(x) = \frac{2\pi}{kK}\sum_{m}^{\infty}\frac{q^{m+\frac{1}{2}}}{1 - q^{2m+1}}\sin\left[(2m+1)\frac{\pi x}{2K}\right] \tag{16}$$

where $q = e^{-\pi(K'/K)}$ is Jacobi's nome. In Eq. (16), K is the complete integral of the first kind of modulus k. Also, K', which appears in the definition of q, is the associated complete integral of the first kind.

Apparent Orbit

From the analytical solution to the restricted tether problem, an equation can be found for the radial distance of m from the Earth in the form of the classical two-body equation. From Eq. (15), this distance is

$$r(\tau) = \frac{k^2 sn^2\left[\sqrt{D}\tau/g + F(\varphi^*, k)\right] - 1}{ck^2 sn^2\left[\sqrt{D}\tau/g + F(\varphi^*, k)\right] - b} r_E \tag{17}$$

With the properties of the elliptic function $sn(\cdot)$ and given that $0 < k^2 < 1$, $c < 0$, and $b > 0$, the maximum and minimum radial distances of the object for restricted tether motion are found to be

$$r_{\max} = (1/b)r_E \tag{18}$$

$$r_{\min} = (k^2 - 1)/(ck^2 - b)r_E \tag{19}$$

These distances may then be used to define an apparent semimajor axis

$$a^* = \frac{1}{2}\left(\frac{1}{b} + \frac{k^2 - 1}{ck^2 - b}\right) r_E \tag{20}$$

and Eq. (20) may be used to derive an apparent eccentricity

$$e^* = \sqrt{1 - h^2/\mu a^*} \tag{21}$$

With the substitution of a^* and e^* in the standard two-body equation for r, an equation for a Keplerian-like orbit is obtained:

$$r_{\text{apparent}} = \frac{a^*(1 - e^{*2})}{1 + e^* \cos\tau} \tag{22}$$

Though this concept of an apparent orbit will not be pursued further; comparison of Eq. (17) with Eq. (22) for several different cases shows that this method can provide a good approximation to restricted tether motion.

Approximate Solution to the Restricted Tether Problem

Although Eq. (15) is an exact solution to the restricted tether motion equations, its form in terms of the elliptic functions limits its usefulness. In some cases approximate solutions may be more convenient in analyzing the dynamic behavior of m. An approximate solution to Eq. (15) can be obtained by applying the general method of averaging.[7] We may rewrite Eq. (7) as

$$u'' + \omega^2 u = 1/h^2 - \varepsilon u^2 \tag{23}$$

where $\omega = \sqrt{[1 + (2/h^2)\varepsilon]}$. If we assume that the solution to Eq. (23) has the form of the solution to the linear term in Eq. (23), then we have

$$u = \gamma\cos(\omega\tau + \xi) + 1/h^2\omega^2 \tag{24}$$

Note that coefficients γ and ξ are variables to be determined to take into account the nonlinear term in Eq. (23). We may derive differential equations for the parameters γ and ξ by using the method of variation of parameters.[7] These equations are

$$\gamma' = \varepsilon[(\gamma^2/\omega)\sin(\omega\tau + \xi)\cos^2(\omega\tau + \xi) + (1/h^4\omega^5)\sin(\omega\tau + \xi) + (2\gamma/h^2\omega^3)\sin(\omega\tau + \xi)\cos(\omega\tau + \xi)] \tag{25}$$

$$\xi' = \varepsilon[(\gamma/\omega)\cos^3(\omega\tau + \xi) + (1/\gamma h^4\omega^5)\cos(\omega\tau + \xi) + (2/h^2\omega^3)\cos^2(\omega\tau + \xi)] \tag{26}$$

Solutions to Eqs. (19) and (20) may be assumed in the forms

$$\gamma = \bar{\gamma} + \varepsilon\tilde{\gamma} \tag{27}$$

$$\xi = \bar{\xi} + \varepsilon\tilde{\xi} \tag{28}$$

where $\bar{\gamma}$ and $\bar{\xi}$ are smoothly varying terms and $\varepsilon\tilde{\gamma}$ and $\varepsilon\tilde{\xi}$ are small harmonic terms. By substituting Eqs. (27) and (28) into Eqs. (25) and (26), averaging over one period $(2\pi/\omega)$, and solving the averaged equations, we get

$$\bar{\gamma} = \gamma_0 \tag{29}$$

$$\bar{\xi} = (\varepsilon/h\omega)\tau + \xi_0 \tag{30}$$

where γ_0 and ξ_0 represent the values these variables take on at $\tau = 0$. Expressions for the oscillatory terms can also be obtained:

$$\tilde{\gamma} = -(\bar{\gamma}^2/4\omega^2)\left[\cos(\omega\tau + \bar{\xi}) + \tfrac{1}{3}\cos 3(\omega\tau + \bar{\xi})\right] - (1/h^4\omega^6) \times \cos(\omega\tau + \bar{\xi}) - (\bar{\gamma}/2h^2\omega^4)\cos 2(\omega\tau + \bar{\xi}) + C_\gamma \tag{31}$$

$$\tilde{\xi} = (\bar{\gamma}^2/4\omega^2)\left[3\sin(\omega\tau + \bar{\xi}) + \tfrac{1}{3}\sin 3(\omega\tau + \bar{\xi})\right] + (1/\bar{\gamma}h^4\omega^6) \times \sin(\omega\tau + \bar{\xi}) + (1/2h^2\omega^4)\sin 2(\omega\tau + \bar{\xi}) + C_\xi \tag{32}$$

The constants of the integration C_γ and C_ξ in Eqs. (31) and (32) are such that $\tilde{\gamma} = \tilde{\xi} = 0$ at $\tau = 0$. That is,

$$C_\gamma = \left(\gamma_0^2/4\omega^2\right)\left(\cos\xi_0 + \tfrac{1}{3}\cos 3\xi_0\right) + (1/h^4\omega^6)\cos\xi_0 + \left(\gamma_0/2h^2\omega^4\right)\cos 2\xi_0 \tag{33}$$

$$C_\xi = -\left(\gamma_0^2/4\omega^2\right)\left(3\sin\xi_0 + \tfrac{1}{3}\sin 3\xi_0\right) - \left(1/\gamma_0 h^4\omega^6\right)\sin\xi_0 - (1/2h^2\omega^4)\sin 2\xi_0 \tag{34}$$

Example results for a TSS orbit are obtained by evaluating both the exact solution [Eq. (15)] and the approximate solution [Eq. (24)] to the restricted tether problem and by numerically integrating Eqs. (4–6). These results are shown in Fig. 2. The initial conditions used are $r_0 = 6621$ km, $\dot{r}_0 = 0$, $\theta_0 = 0$, $\dot{\theta}_0 = 1.1835E{-}3$ rad/s, tether length = 10 km, mass ratio $m/m_p = 0.1$, and tether parameter $\varepsilon = 1.4254E{-}3$. The parameters a, b, and c from Eq. (11) are the zeros of the cubic function that appears under the radical in Eq. (10).

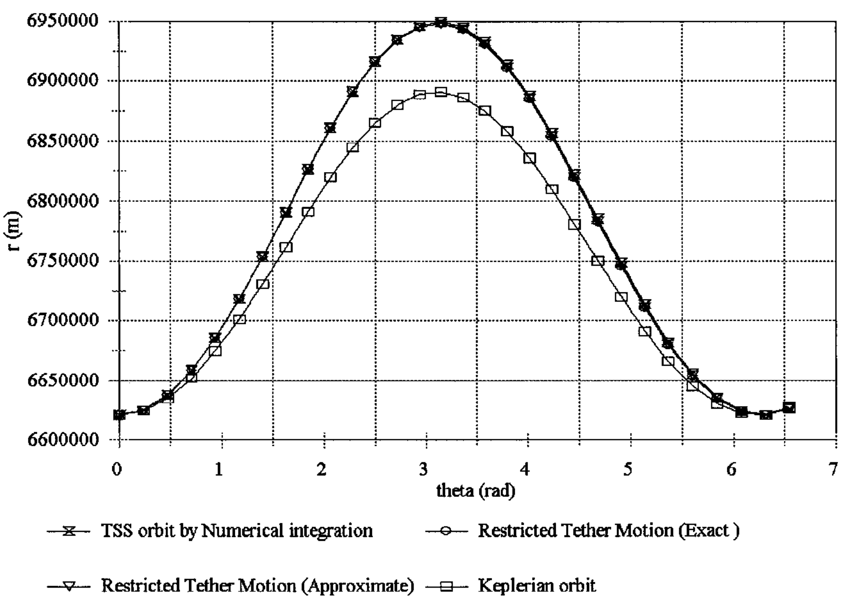

Fig. 2 Comparison of solutions for TSS orbital radius.

In this example they are given by $a = 1.5103E{-}7$, $b = 1.4392E{-}7$, and $c = -1.6574E{-}4$. Also, the values of γ_0 and ξ_0 are determined by evaluating Eq. (24) and its derivative at $\tau = 0$ and applying the initial conditions on u and u'. For this case, $\gamma_0 = 2.1424E{-}2$ and $\xi_0 = 0.0$.

That all three of the aforementioned curves lie practically on top of one another demonstrates that both the exact and approximate solutions to the restricted tether problem are very good approximations to the TSS orbit solution obtained by numerical integration. The result for a Keplerian orbit with the same initial conditions is provided in Fig. 2 as well, to show how it differs from the tether-perturbed orbit.

IV. Relative Motion of the Tethered Mass

Relative motion of the tethered satellite m_p is described by Eq. (6), which is a second-order differential equation with a small nonlinear term. Note that Eq. (5) can be rearranged as

$$h'/h = \varepsilon\left[u(\theta_3' + 1)^2 + 2/h^2\right]\theta_3 \tag{35}$$

and inserted into Eq. (6) to give

$$\theta_3'' = -(2u'/u)(\theta_3' + 1) - (3/h^2 u)\theta_3 - (h'/h)(\theta_3' + 1) \tag{36}$$

Because the orbital motion approximation is based on $h' = 0$, it is consistent to neglect the last term on the right-hand side in the process of finding an approximate solution for θ_3. The solution will be zeroth order in ε and, thus, will not depend on the tether length. Equation (6) then becomes a second-order, nonhomogeneous, linear differential equation with variable coefficients:

$$\theta_3'' + 2P(\tau)\theta_3' + R^2(\tau)\theta_3 = Q(\tau) \tag{37}$$

where

$$P(\tau) = u'/u \tag{38}$$

$$R(\tau)^2 = 3/h^2 u \tag{39}$$

$$Q(\tau) = -2(u'/u) \tag{40}$$

In Eqs. (38–40), equations for u and u' may be expressed by the zeroth-order (in ε) solution in Eq. (24). They are

$$u \approx \gamma_0 \cos(\omega\tau + \xi_0) + 1/h^2\omega^2 \tag{41}$$

$$u' \approx -\omega\gamma_0 \sin(\omega\tau + \xi_0) \tag{42}$$

To solve Eq. (37), first the variable θ_3 is transformed to a new variable ϕ, which is defined by

$$\varphi = \theta_3 \exp\left[\int P(\tau)\,\mathrm{d}\tau\right] = \theta_3 u \tag{43}$$

or

$$\theta_3 = \varphi \exp\left[\int -P(\tau)\,\mathrm{d}\tau\right] = \frac{\varphi}{u} \tag{44}$$

Then Eq. (37) can be expressed in the simpler form

$$\varphi'' + G(\tau)^2\varphi = Q^*(\tau) \tag{45}$$

where

$$G(\tau)^2 = R^2 - P^2 - P' \tag{46}$$

$$Q^*(\tau) = Q(\tau)\exp\left[\int P\,\mathrm{d}\tau\right] = -2u' \tag{47}$$

By substituting Eqs. (41) and (42) into Eqs. (38–40) and (46), using a Taylor series expansion for G about $\gamma_0 = 0$, and neglecting terms of order γ_0^2 or higher, we obtain the following expression:

$$G(\tau) \approx \Omega_0\left[1 - \tfrac{1}{3}h^2\omega^2\gamma_0\cos(\omega\tau + \xi_0)\right] \tag{48}$$

where $\Omega_0 = \omega\sqrt{3}$. Because G executes small changes about its mean value Ω_0, the Wentzel-Kramers-Brillouin-Jeffreys approximation[8] can be used to obtain the following two linearly independent homogeneous solutions to Eq. (45):

$$x_1 = \left(1/\sqrt{G}\right)\cos\zeta \tag{49}$$

$$x_2 = \left(1/\sqrt{G}\right)\sin\zeta \tag{50}$$

where

$$\zeta(\tau) = \int G\,\mathrm{d}\tau \tag{51}$$

Using the method of variation of parameters, we seek a particular solution of the form

$$\varphi(\tau) = \alpha x_1 + \beta x_2 \tag{52}$$

where α and β must satisfy

$$\alpha' = \frac{-Q^* x_2}{x_1 x_2' - x_2 x_1'} \tag{53}$$

$$\beta' = \frac{Q^* x_1}{x_1 x_2' - x_2 x_1'} \tag{54}$$

By integrating Eqs. (53) and (54), we obtain the following solutions for α and β (again, neglecting terms of order γ_0^2 or higher):

$$\alpha = -\frac{\omega\gamma_0}{\sqrt{\Omega_0}}\left\{\frac{[\sin(\omega - \Omega_0)]\tau + \xi_0}{\omega - \Omega_0} - \frac{[\sin(\omega + \Omega_0)\tau + \xi_0]}{\omega + \Omega_0}\right\} + C_\alpha \tag{55}$$

$$\beta = -\frac{\omega\gamma_0}{\sqrt{\Omega_0}}\left\{\frac{[\cos(\omega - \Omega_0)\tau + \xi_0]}{\omega - \Omega_0} + \frac{[\cos(\omega + \Omega_0)\tau + \xi_0]}{\omega + \Omega_0}\right\} + C_\beta \tag{56}$$

where the constants of integration C_α and C_β are chosen such that

$$\varphi(0) = \alpha(0)x_1(0) + \beta(0)x_2(0) = \theta_3(0)u(0) \tag{57}$$

and

$$\begin{aligned}\varphi'(0) &= \alpha'(0)x_1(0) + \alpha(0)x_1'(0) + \beta'(0)x_2(0) + \beta(0)x_2'(0)\\ &= \theta_3'(0)u(0) + \theta_3(0)u'(0)\end{aligned} \tag{58}$$

Finally, we may find the solution for θ_3 by substituting ϕ into Eq. (44):

$$\theta_3 = (\alpha x_1 + \beta x_2)(1/u) \tag{59}$$

Note that the preceding solution is valid only for near-circular orbits. This is because the effect of γ in Eq. (24) is to add eccentricity to the circular orbit, and in the foregoing analysis γ was assumed to be small. Results obtained from the analytical solution in Eq. (59) are compared with numerical simulation results in Fig. 3. The same initial conditions for the results in Fig. 2 were used to obtain Fig. 3. It is seen that the results from the approximate analytical solution to the librational motion match those from the numerical simulation very well; in fact, the maximum difference in the value of θ_3 obtained by the two methods is less than 0.002 rad. Thus, for small eccentricities and small libration amplitude, the analytical solution may be used to predict accurately libration of a tether-connected satellite system.

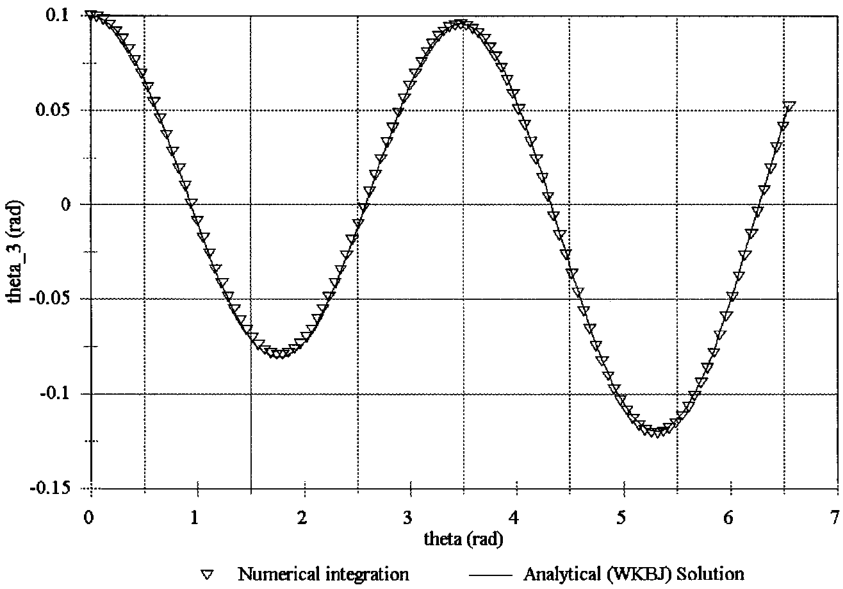

Fig. 3 Comparison of solutions for librational motion.

V. Identification of a TSS

The solutions obtained in this paper may be useful in predicting the orbital motion and libration of a two-satellite tethered system. Here a solution to the identification problem is posed by using equations for the restricted tether motion. In Refs. 2 and 3, a state estimation process to identify a TSS by observing only one of the satellites in the TSS was tested. Difficulties encountered in Refs. 2 and 3 were 1) that the state estimation process, including states for the libration angle, fails when a short observation period is used; 2) that very accurate guesses for the initial states, which must be determined by a preliminary orbit determination process, are needed for successful convergence; and 3) that initial states for the libration angle cannot be obtained a priori. These problems are caused by the lack of direct information on the librational motion provided in the observations and because the effects of libration on the observed satellite are often very small.

The success of the identification process seems to require a tradeoff between performance in detecting the effect of the tether force on the observed satellite and achieving completeness of system identification. If detection is the main objective, neglecting states that govern the librational motion should be acceptable, provided the libration is small in amplitude and/or the tether length is small, for example, less than 20 km. It follows that ignoring the libration states in the equations of motion may improve the performance of an estimator without a significant loss of accuracy. In Fig. 2, it was shown that the equations of motion with zero libration described the orbital motion of a two-satellite tethered system very well in cases of small amplitude librational motion. Thus, by ignoring the states about which we have little information, we may eliminate some difficulties.

A method of identification of a TSS based on the aforementioned consideration is proposed. In this process, the equations for the restricted tether motion are used in a batch filter. The method is constructed in three stages similar to the method used in Ref. 9. First, a state estimation technique using the equations for two-body motion is applied with limited observation data. Only one of the satellites in a tethered system is observed and the observation period is limited to a short arc. The state vector to be estimated in the first stage is

$$X = [r \quad \theta \quad \dot{r} \quad \dot{\theta} \quad \mu]^T \tag{60}$$

In Eq. (60), r is radial distance and θ is true anomaly. From this first stage, three different results are expected. If the observed satellite is a single satellite, the states should be estimated with high accuracy. This can be verified by comparing the estimated value of μ with the true gravitational constant. If the observed satellite is a member of a TSS, then the estimation process may be successful or not. That is, although the procedure estimates the state vector successfully, the results may be in error. An estimated gravitational constant may be used to detect errors in results. If the process fails to converge, the observed satellite may be a member of a TSS for which the dynamics of two-body motion is not a good model. For all of the preceding cases, more steps are needed to complete the identification.

Equations for the restricted tether motion are applied in the second stage to verify and improve the results. The restricted tether motion describes the gross orbital motion of a TSS. As mentioned earlier, neglecting the librational motion provides an advantage in the estimation process.

If the states are estimated successfully in the first stage, these estimates may be used as an initial guess of the second stage. The state vector for the restricted tether motion is

$$X = [r \quad \theta \quad \dot{r} \quad \dot{\theta} \quad \varepsilon]^T \tag{61}$$

where ε is the tether parameter. The tether parameter can be obtained from the first-stage results because we can write[2,10]

$$\varepsilon \approx (r_0/r_E)(\mu - \mu_e)/(\mu_e + 2\mu) \tag{62}$$

where μ_e is the estimated value for the gravitational constant. If the second stage is successfully finished, the estimated state vector identifies a TSS more completely.

The third stage employs the two-dimensional motion of a TSS, that is, the state vector contains the in-plane librational variables. Thus, the state vector is defined as

$$X = [r \quad \theta \quad \theta_3 \quad \dot{r} \quad \dot{\theta} \quad \dot{\theta}_3 \quad \varepsilon]^T \tag{63}$$

where θ_3 is the in-plane libration angle. Although this stage may not always be necessary for identification of a TSS, it completes the identification with higher confidence.

To illustrate this identification process, several circular and elliptical orbit conditions, with and without libration, were chosen. Table 1 provides parameters and initial conditions for 10 different cases. Initial (nondimensional) radial distance for all cases is 1.047. For the cases C, initial osculating eccentricity is zero, whereas the cases E have an eccentricity of 0.2. Cases C-1 and C-2, representing circular orbits of m and m_p without librational motion, were obtained by applying the circular equilibrium angular rate (given in the fifth column of Table 1). Cases C-3 and C-4 are examples of small in-plane libration, one having a larger tether parameter than the other. Cases C-5 and C-6 include large in-plane libration for the same tether parameters as in cases C-3 and C-4, respectively. Cases E-3–E-6 are similar to cases C-3–C-6, except that the initial

Table 1 Example cases

Case	m_p/m	ρ, km	ε	$\dot{\theta}_0$	θ_{30}
C-1	1.0	10	7.8394E−04	9.3233E−01	0.0
C-2	10.0	100	1.4254E−02	9.1438E−01	0.0
C-3	1.0	10	7.8394E−04	9.3128E−01	0.1
C-4	10.0	100	1.4254E−02	9.1280E−01	0.1
C-5	1.0	10	7.8394E−04	9.3128E−01	1.0
C-6	10.0	100	1.4254E−02	9.1280E−01	1.0
E-3	1.0	10	7.8394E−04	1.0202E+00	0.1
E-4	10.0	100	1.4254E−02	9.9992E−01	0.1
E-5	1.0	10	7.8394E−04	1.0202E+00	1.0
E-6	10.0	100	1.4254E−02	9.9992E−01	1.0

angular rate is that which provides an eccentricity of 0.2. All data were generated by numerical integration of the equations for complete three-dimensional motion. The observation period is about 1/16 of the orbital period. Data points were collected every 5 s, for a total of about 70 data points. Tables 2–11 show results of the identification process via the three-stage method; the stages are labeled two-body motion, restricted motion, and plane TSS, respectively. Values are all in nondimensional units except for the gravitational constant μ which is expressed in units of km^3/s^2.

In case C-1 (Table 2), the first stage converges, with the estimated gravitational constant indicating a possible tethered satellite. Therefore, the second stage is performed and verifies the tethered satellite motion of the object. The results of the third stage show estimated

Table 2 Estimation results for case C-1

		Two-body motion model		Restricted motion model		Plane TSS model	
Parameter	True state	Guess	Result	Guess	Result	Guess	Result
r	1.047E+00	1.000E+00	1.047E+00	1.047E+00	1.047E+00	1.047E+00	1.047E+00
θ	3.491E−01	0.000E+00	3.491E−01	3.491E−01	3.491E−01	3.491E−01	3.491E−01
$\dot{r}$	0.000E+00	0.000E+00	8.604E−16	8.604E−16	−3.268E−10	0.000E+00	2.801E−13
$\dot{\theta}$	9.323E−01	1.000E+00	9.323E−01	9.323E−01	9.323E−01	9.323E−01	9.323E−01
θ_3	0.000E+00	——	——	——	——	0.000E+00	8.269E−05
$\dot{\theta}_3$	0.000E+00	——	——	——	——	9.323E−01	−4.040E−04
ε	7.839E−04	——	7.834E−04	7.833E−04	7.839E−04	7.840E−04	7.842E−04
μ	3.986E+14	3.986E+14	3.977E+14	——	——	——	——

Table 3 Estimation results for case C-2

		Two-body motion model		Restricted motion model		Plane TSS model	
Parameter	True state	Guess	Result	Guess	Result	Guess	Result
r	1.047E+00	1.000E+00	1.047E+00	1.047E+00	1.047E+00	1.047E+00	1.047E+00
θ	3.491E−01	0.000E+00	3.491E−01	3.491E−01	3.491E−01	3.491E−01	3.491E−01
$\dot{r}$	0.000E+00	1.000E−01	−7.597E−16	0.000E+00	1.350E−09	0.000E+00	7.610E−11
$\dot{\theta}$	9.144E−01	1.000E+00	9.144E−01	9.144E−01	9.144E−01	9.144E−01	9.144E−01
θ_3	0.000E+00	——	——	——	——	1.000E+00	−1.580E−05
$\dot{\theta}_3$	0.000E+00	——	——	——	——	9.144E−01	6.613E−05
ε	1.425E−02	——	1.425E−02	1.425E−02	1.425E−02	1.425E−02	1.425E−02
μ	3.986E+14	3.986E+14	3.825E+14	——	——	——	——

Table 4 Estimation results for case C-3

		Two-body motion model		Restricted motion model		Plane TSS model	
Parameter	True state	Guess	Result	Guess	Result	Guess	Result
r	1.047E+00	1.000E+00	1.047E+00	1.047E+00	1.047E+00	1.047E+00	1.047E+00
θ	3.491E−01	0.000E+00	3.352E−01	3.352E−01	3.491E−01	3.491E−01	3.491E−01
$\dot{r}$	0.000E+00	0.000E+00	2.825E−07	2.825E−07	−1.423E−06	0.000E+00	1.081E−07
$\dot{\theta}$	9.313E−01	1.000E+00	9.960E−01	9.960E−01	9.313E−01	9.313E−01	9.313E−01
θ_3	1.000E−01	——	——	——	——	1.000E+00	1.010E−01
$\dot{\theta}_3$	0.000E+00	——	——	——	——	9.313E−01	−4.453E−03
ε	7.839E−04	——	−4.702E−02	−4.702E−02	7.447E−04	7.447E−04	7.864E−04
μ	3.986E+14	3.986E+14	4.548E+14	——	——	——	——

Table 5 Estimation results for case C-4

		Two-body motion model		Restricted motion model		Plane TSS model	
Parameter	True state	Guess	Result	Guess	Result	Guess	Result
r	1.047E+00	1.000E+00	——	1.000E+00	1.047E+00	1.047E+00	1.047E+00
θ	3.491E−01	0.000E+00	——	0.000E+00	3.490E−01	3.490E−01	3.491E−01
$\dot{r}$	0.000E+00	1.000E−01	——	0.000E+00	−2.545E−05	1.000E−04	−2.686E−08
$\dot{\theta}$	9.128E−01	1.000E+00	——	1.000E+00	9.135E−01	9.135E−01	9.128E−01
θ_3	1.000E−01	——	Failed	——	——	1.000E−00	1.000E−01
$\dot{\theta}_3$	0.000E+00	——	——	——	——	9.135E−01	−7.388E−05
ε	1.425E−02	——	——	1.000E−03	1.353E−02	1.353E−02	1.425E−02
μ	3.986E+14	3.986E+14	——	——	——	——	——

Table 6 Estimation results for case C-5

		Two-body motion model		Restricted motion model		Plane TSS model	
Parameter	True state	Guess	Result	Guess	Result	Guess	Result
r	$1.047E+00$	$1.000E+00$	$1.047E+00$	$1.047E+00$	$1.047E+00$	$1.047E+00$	$1.047E+00$
θ	$3.491E-01$	$0.000E+00$	$3.312E-01$	$3.312E-01$	$3.491E-01$	$3.491E-01$	$3.491E-01$
$\dot{r}$	$0.000E+00$	$0.000E+00$	$3.755E-07$	$0.000E+00$	$-3.132E-6$	$-3.132E-6$	$7.577E-08$
$\dot{\theta}$	$9.313E-01$	$1.000E+00$	$1.015E+00$	$1.015E+00$	$9.314E-01$	$9.314E-01$	$9.313E-01$
θ_3	$1.000E+00$	——	——	——	——	$1.000E-01$	$1.001E+00$
$\dot{\theta}_3$	$0.000E+00$	——	——	——	——	$9.314E-01$	$3.854E-03$
ε	$7.839E-04$	——	$-6.510E-2$	$-6.510E-2$	$7.394E-05$	$7.394E-05$	$7.801E-04$
μ	$3.986E+14$	$3.986E+14$	$4.729E+14$	——	——	——	——

Table 7 Estimation results for case C-6

		Two-body motion model		Restricted motion model		Plane TSS model	
Parameter	True state	Guess	Result	Guess	Result	Guess	Result
r	$1.047E+00$	$1.000E+00$	$1.047E+00$	$1.047E+00$	$1.047E+00$	$1.047E+00$	$1.047E+00$
θ	$3.491E-01$	$0.000E+00$	$3.150E-01$	$3.150E-01$	$3.490E-01$	$3.490E-01$	$3.491E-01$
$\dot{r}$	$0.000E+00$	$1.000E-01$	$1.097E-05$	$1.097E-05$	$-5.082E-5$	$-5.082E-5$	$7.698E-08$
$\dot{\theta}$	$9.128E-01$	$1.000E+00$	$1.070E+00$	$1.070E+00$	$9.141E-01$	$9.141E-01$	$9.128E-01$
θ_3	$1.000E+00$	——	——	——	——	$1.000E-01$	$1.000E+00$
$\dot{\theta}_3$	$0.000E+00$	——	——	——	——	$9.141E-01$	$-2.598E-04$
ε	$1.425E-02$	——	$-1.231E-1$	$-1.231E-1$	$1.280E-03$	$1.280E-03$	$1.427E-02$
μ	$3.986E+14$	$3.986E+14$	$5.392E+14$	——	——	——	——

Table 8 Estimation results for case E-3

		Two-body motion model		Restricted motion model		Plane TSS model	
Parameter	True state	Guess	Result	Guess	Result	Guess	Result
r	$1.047E+00$	$1.000E+00$	$1.047E+00$	$1.047E+00$	$1.047E+00$	$1.047E+00$	$1.047E+00$
θ	$3.491E-01$	$0.000E+00$	$3.492E-01$	$3.492E-01$	$3.491E-01$	$3.491E-01$	$3.491E-01$
$\dot{r}$	$0.000E+00$	$0.000E+00$	$-3.179E-07$	$-3.179E-07$	$-7.721E-06$	$-7.721E-6$	$7.566E-08$
$\dot{\theta}$	$1.020E+00$	$1.000E+00$	$1.020E+00$	$1.020E+00$	$1.020E+00$	$1.020E+00$	$1.020E+00$
θ_3	$1.000E-01$	——	——	——	——	$1.000E+00$	$1.001E-01$
$\dot{\theta}_3$	$0.000E+00$	——	——	——	——	$1.020E+00$	$-1.997E-04$
ε	$7.839E-04$	——	$1.256E-03$	$1.256E-03$	$7.441E-04$	$7.441E-04$	$7.840E-04$
μ	$3.986E+14$	$3.986E+14$	$3.971E+14$	——	——	——	——

Table 9 Estimation results for case E-4

		Two-body motion model		Restricted motion model		Plane TSS model	
Parameter	True state	Guess	Result	Guess	Result	Guess	Result
r	$1.047E+00$	$1.000E+00$	$1.047E+00$	$1.047E+00$	$1.047E+00$	$1.047E+00$	——
θ	$3.491E-01$	$0.000E+00$	$3.519E-01$	$3.519E-01$	$3.490E-01$	$3.490E-01$	——
$\dot{r}$	$0.000E+00$	$1.000E-01$	$-6.280E-06$	$-6.280E-06$	$-1.387E-04$	$-1.387E-04$	——
$\dot{\theta}$	$9.999E-01$	$1.000E+00$	$9.913E-01$	$9.913E-01$	$1.001E+00$	$1.001E+00$	——
θ_3	$1.000E-01$	——	——	——	——	$1.000E+00$	——
$\dot{\theta}_3$	$0.000E+00$	——	——	——	——	$1.001E+00$	——
ε	$1.425E-02$	——	$2.166E-02$	$2.166E-02$	$1.351E-02$	$1.351E-02$	——
μ	$3.986E+14$	$3.986E+14$	$3.738E+14$	——	——	——	——

Table 10 Estimation results for case E-5

		Two-body motion model		Restricted motion model		Plane TSS model	
Parameter	True state	Guess	Result	Guess	Result	Guess	Result
r	$1.047E+00$	$1.000E+00$	$1.047E+00$	$1.047E+00$	$1.047E+00$	$1.047E+00$	$1.047E+00$
θ	$3.491E-01$	$0.000E+00$	$3.502E-01$	$3.502E-01$	$3.491E-01$	$3.491E-01$	$3.491E-01$
$\dot{r}$	$0.000E+00$	$1.000E-01$	$-8.798E-07$	$-8.798E-07$	$-1.577E-05$	$-1.577E-5$	$-1.723E-07$
$\dot{\theta}$	$1.020E+00$	$1.000E+00$	$1.017E+00$	$1.017E+00$	$1.020E+00$	$1.020E+00$	$1.020E+00$
θ_3	$1.000E+00$	——	——	——	——	$5.000E-01$	$9.986E-01$
$\dot{\theta}_3$	$0.000E+00$	——	——	——	——	$1.020E+00$	$2.046E-03$
ε	$7.839E-04$	——	$3.157E-03$	$3.157E-03$	$8.525E-05$	$8.525E-05$	$7.776E-04$
μ	$3.986E+14$	$3.986E+14$	$3.949E+14$	——	——	——	——

Table 11 Estimation results for case E-6

		Two-body motion model		Restricted motion model		Plane TSS model	
Parameter	True state	Guess	Result	Guess	Result	Guess	Result
r	$1.047E+00$	$1.000E+00$	$1.047E+00$	$1.047E+00$	$1.047E+00$	$1.047E+00$	$1.047E+00$
θ	$3.491E-01$	$0.000E+00$	$3.755E-01$	$3.755E-01$	$3.489E-01$	$3.489E-01$	$3.491E-01$
$\dot{r}$	$0.000E+00$	$1.000E-01$	$-3.255E-07$	$-3.225E-07$	$-2.721E-04$	$-2.721E-04$	$-1.283E-7$
$\dot{\theta}$	$9.999E-01$	$1.000E+00$	$9.135E-01$	$9.135E-01$	$1.002E+00$	$1.002E+00$	$9.999E-01$
θ_3	$1.000E+00$	——	——	——	——	$1.000E-01$	$9.999E-01$
$\dot{\theta}_3$	$0.000E+00$	——	——	——	——	$1.002E+00$	$2.962E-05$
ε	$1.425E-02$	——	$6.891E-02$	$6.891E-02$	$1.478E-03$	$1.478E-03$	$1.425E-02$
μ	$3.986E+14$	$3.986E+14$	$3.199E+14$	——	——	——	——

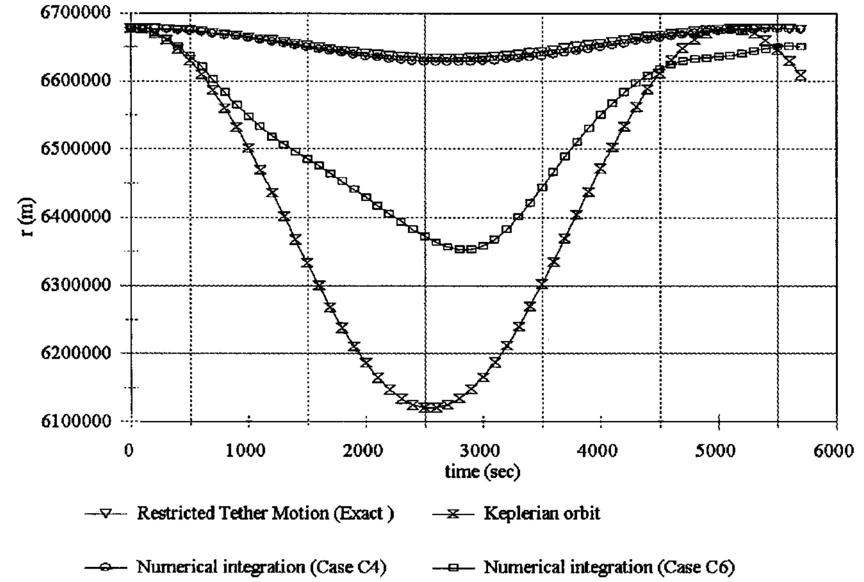

Fig. 4 Radial distance for near-circular orbit and large tether parameters.

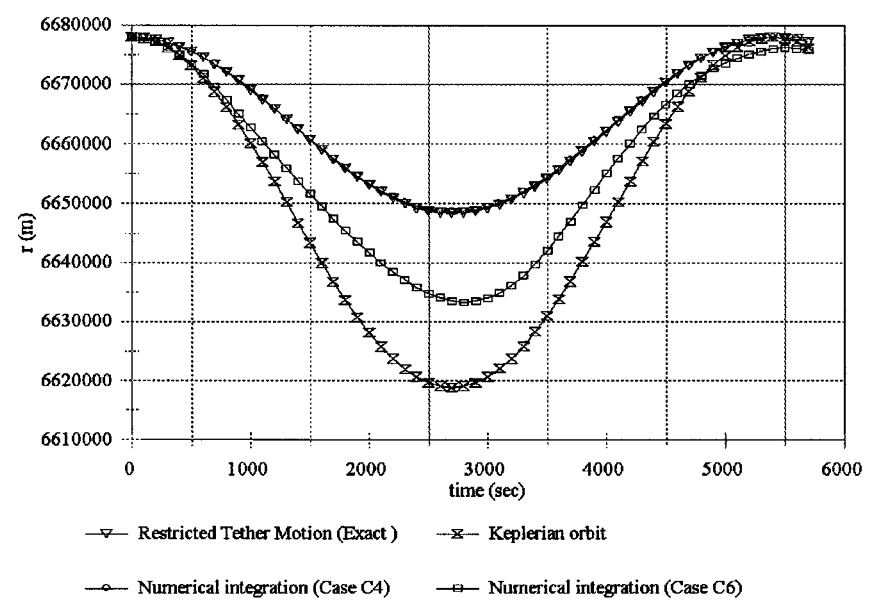

Fig. 5 Radial distance for near-circular orbit and small tether parameters.

values of the librational states as well. Table 3 presents case C-2, for which identification is similarly successful.

Case C-3 (Table 4) includes small libration. For this case, the first stage cannot provide a good estimate of the tether parameter. However, the second stage provides accurate estimates of ε and of the restricted tether motion states. The third stage then provides very good estimates of all states.

In case C-4 (Table 5), the first stage estimation process failed. This is likely because the effect of the tether caused the mass to deviate too much from two-body motion. This is illustrated in Fig. 4, which presents simulation results of cases C-4, C-6, restricted tether motion, and two-body motion. (In all cases, the initial radius, orbital angle, and angular rate are the same.) In Fig. 4, it is clear that C-4 cannot be tracked well at all by using equations for two-body motion. By contrast, Fig. 5 shows results for the cases with much smaller tether parameters. Although two-body motion is not necessarily close to the motion of C-3, the magnitude of the difference is much smaller than in Fig. 4.

In cases C-5 and C-6 (Tables 6 and 7), all states in the first-stage process are estimated successfully except for the value of μ; in the second stage, the value of μ is greatly refined. Finally, in the third stage, all states in the two-dimensional motion of the TSS are successfully estimated, including librational motion.

Tables 8–11 present estimation results for cases E-3–E-6. For each of these cases, the success of all three stages of the identification process is equal to or better than that of the near-circular case with the same tether parameter and initial libration, that is cases C-3–C-6, with the lone exception that the third-stage process fails for case E-4.

VI. Conclusions

Approximate analytical solutions to the equations of planar motion of a two-satellite tethered system have been obtained. An exact solution to a restricted tether problem obtained by neglecting libration was found in terms of elliptic functions and integrals. This solution provides results that agree very well with exact results obtained by numerically integrating the complete equations for the two-satellite tethered system. The concept of an apparent orbit, which is a projection of the tethered satellite motion onto a Keplerian orbit, was also discussed. An approximate solution to the restricted tether problem was also found by applying the general method of averaging. A solution to the equation that governs librational motion was then found. The solutions derived in this work provide considerable insight regarding the principal motion of tethered satellite systems.

The three-stage method proposed for identification was used to obtain definitive results for several different cases of tethered satellite motion. It was shown that this method can be used successfully when only a short period of observation time and relatively imprecise initial state information are available. The restricted tether motion model may prove useful in addressing the state estimation problem for tethered satellite systems because this model is a good approximation to the orbit of a two-satellite tethered system and it neglects the libration that causes numerical problems in the estimation process.

Acknowledgments

This work was partially supported by the Air Force Office of Scientific Research under Contract AF-F49670-97-1-0539. The authors wish to thank R. Racca and J. Liu for their input regarding this work.

References

[1]Beletsky, V. V., and Levin, E. V., *Dynamics of Space Tether Systems*, Vol. 83, Advances in the Astronautical Sciences, American Astronautical Society, San Diego, CA, 1993, p. 76.

[2]Cho, S., Cochran, J. E., Jr., and Cicci, D. A., "Identification and Orbit Determination of Tethered Satellite System," American Astronautical Society Paper 98-101, Feb. 1998.

[3]Cochran, J. E., Jr., Cho, S., Lovell, A., and Cicci, D. A., "On the Information Contained in the Motion of One Satellite of a Two-Satellite Tethered System," *Journal of Astronautical Sciences* (submitted for publication).

[4]Von Flotow, A. H., "Some Approximations for the Dynamics of Spacecraft Tethers," AIAA Paper 87-0821, April 1987.

[5]Nacozy, P. E., "Dynamics Analysis of Electrodynamic Satellite Tethers. Equations of Motion and Numerical Solution Algorithms for the Tether," NASA CR-171777, Jan. 1984.

[6]Byrd, P. F., and Friedman, M. D., *Handbook of Elliptic Integrals for Engineers and Scientists*, 2nd Ed., Springer-Verlag, New York, 1971, p. 77.

[7]Sanders, J. A., and Verhulst, F., *Averaging Methods in Nonlinear Dynamical Systems*, Springer-Verlag, New York, 1985, pp. 207–210.

[8]Cunningham, W. J., *Introduction to Nonlinear Analysis*, McGraw–Hill, New York, 1958, pp. 253, 254.

[9]Cho, S., "Analysis of Orbital Motion of a Tethered Satellite System," Ph.D. Dissertation, Dept. of Aerospace Engineering, Auburn Univ., Auburn, AL, June 1999.

[10]Cochran, J. E., Jr., Cho, S., Cheng, Y-M., and Cicci, D. A., "Dynamics and Orbit Determination of Tethered Satellite Systems," *Journal of Astronautical Sciences*, Vol. 48, No. 2, 1998, pp. 177–194.